Pesq. Vet. Bras. 46:e07823, 2026
DOI: 10.1590/1678-5150-PVB-7823

Original Article
Small Animal Diseases

Applicability of acoustic radiation force impulse (ARFI) elastography in the evaluation of the pneumopleural interface in dogs with myxomatous mitral valve disease[1]

Brenda S.P. Miranda[2]*, Bruna B. Lima[2], Rafael K. Carneiro[3], Danuta P. Doiche[2], Giovanna S.M. Feliciano[4], Gabriela C.L. Evangelista[4], Ricardo A.R. Uscategui[5], Marcus Antônio R. Feliciano[2,4]

Registros ORCID:
Brenda Santos Pompeu de Miranda – https://orcid.org/0000-0001-9064-4309
Bruna Bressianini Lima – https://orcid.org/0000-0003-4158-9109
Rafael Kretzer Carneiro – https://orcid.org/0000-0002-1121-0981
Danuta Pulz Doiche – https://orcid.org/0000-0002-3273-0142
Giovanna Serpa Maciel Feliciano – https://orcid.org/0000-0003-3628-2989
Gabriela Castro Lopes Evangelista – https://orcid.org/0000-0001-9699-7172
Ricardo Andrés Ramirez Uscategui – https://orcid.org/0000-0002-9760-8631
Marcus Antônio Rossi Feliciano – https://orcid.org/0000-0003-4373-6539

ABSTRACT.- Miranda BSP, Lima BB, Carneiro RK, Doiche DP, Feliciano GSM, Evangelista GCL, Uscategui RAR, Feliciano MAR. **Applicability of acoustic radiation force impulse (ARFI) elastography in the evaluation of the pneumopleural interface in dogs with myxomatous mitral valve disease**. *Pesquisa Veterinária Brasileira 46:e07823, 2026.* Universidade de São Paulo, Faculdade de Zootecnia e Engenharia de Alimentos, Rua Duque de Caxias 225, Jardim Elite, Pirassununga, SP 13635-000, Brazil. E-mail: brenda.pompeu@unesp.br

Myxomatous mitral valve disease (MMVD) is the most common heart disease in dogs, causing mitral valve degeneration that can lead to heart failure and, in advanced cases, collapse or sudden death, as well as secondary pulmonary changes such as pulmonary congestion and edema. A prospective, case-control, and observational study was conducted to evaluate the utility of B-mode ultrasonography and acoustic radiation force impulse (ARFI) elastography for assessing the pleuropulmonary interface in dogs with MMVD. Fifteen dogs with MMVD (American College of Veterinary Internal Medicine – ACVIM stages B1, B2, and C) and fifteen healthy dogs underwent radiographic, echocardiographic, and ultrasonographic examinations, including the VetBLUE protocol. While B-lines were infrequently observed, quantitative ARFI elastography revealed a significant reduction in shear wave velocity (SWV) in the perihilar, medial, and cranial lung regions of the MMVD group, indicating decreased tissue stiffness. Furthermore, pleural thickness was significantly greater in sick animals. A mean SWV cutoff value of < 3.71 m/s demonstrated high sensitivity (80%) and specificity (86.67%) for identifying dogs with MMVD. Elastography detected structural changes at the pleuropulmonary interface associated with MMVD, with ARFI proving a more sensitive, non-invasive tool than B-mode for early detection.

INDEX TERMS: Shear wave, lung, canine heart disease, pleura, ultrasound.

[1] Received on March 10, 2026.
Accepted for publication on May 8, 2026.

[2] Departamento de Clínica e Cirurgia Veterinária, Faculdade de Ciências Agrárias e Veterinárias (FCAV), Universidade Estadual Paulista "Júlio de Mesquita Filho" (Unesp), Campus de Jaboticabal, Via de Acesso Prof. Paulo Donato Castelane Castellane s/n, Vila Industrial, Jaboticabal, SP 14884-900, Brazil. *Corresponding author: brenda.pompeu@unesp.br

[3] Departamento de Medicina Veterinária, Centro de Ciências Agroveterinárias (CAV), Universidade do Estado de Santa Catarina (UDESC), Av. Luiz de Camões 2090, Bairro Conta Dinheiro, Lages, SC 88520-000, Brazil.

[4] Departamento de Medicina Veterinária, Faculdade de Zootecnia e Engenharia de Alimentos (FZEA), Universidade de São Paulo (USP), Rua Duque de Caxias 225, Jardim Elite, Pirassununga, SP 13635-900, Brazil.

[5] Departamento de Sanidad Animal, Facultad de Medicina Veterinaria y Zootecnia, Universidad del Tolima, Barrio Santa Helena, Parte Alta I, Código Postal 730006299, Ibagué, Tolima, Colombia.

RESUMO.- [**Aplicabilidade da elastografia por impulso de força de radiação acústica (ARFI) na avaliação da interface pneumopleural em cães com doença mixomatosa da valva mitral.**] A doença mixomatosa da valva mitral (DMVM) é a doença cardíaca mais comum em cães, causando degeneração da valva mitral que pode levar à insuficiência cardíaca e, em casos avançados, ao colapso ou à morte súbita, bem como a alterações pulmonares secundárias, como congestão pulmonar e edema. Um estudo prospectivo, caso-controle e observacional foi conduzido para avaliar a utilidade da ultrassonografia em modo B e da elastografia por impulso de força de radiação acústica (ARFI) na avaliação da interface pleuropulmonar em cães com DMVM. Quinze cães com DMVM (estágios B1, B2 e C do "American College of Veterinary Internal Medicine" – ACVIM) e quinze cães saudáveis foram submetidos a exames radiográficos, ecocardiográficos e ultrassonográficos, incluindo o protocolo VetBLUE. Embora as linhas B tenham sido observadas com pouca frequência, a elastografia ARFI quantitativa revelou uma redução significativa na velocidade da onda de cisalhamento (SWV) nas regiões peri-hilares, mediais e craniais do pulmão no grupo com DMVM, indicando diminuição da rigidez tecidual. Além disso, a espessura pleural foi significativamente maior nos animais doentes. Um valor médio de corte de SWV < 3,71 m/s apresentou alta sensibilidade (80%) e especificidade (86,67%) para identificar cães com DMVM. A elastografia detectou alterações estruturais na interface pleuropulmonar associadas à DMVM, sendo a ARFI uma ferramenta não invasiva mais sensível do que o modo B para detecção precoce.

TERMOS DE INDEXAÇÃO: Onda de cisalhamento, pulmão, doença cardíaca canina, pleura, ultrassom.

INTRODUCTION

Approximately 10% of dogs presented to veterinary clinics suffer from some form of heart disease, with myxomatous mitral valve disease (MMVD), also known as mitral endocardiosis, accounting for approximately 75% of these cases in North American veterinary practices (Keene et al. 2019). The mechanical alterations caused by valvular lesions lead to cardiovascular dysfunction, resulting from the heart's compensatory mechanisms that attempt to maintain cardiac output. These adaptations include left atrial enlargement, eccentric hypertrophy of the left ventricle due to volume overload, activation of the renin-angiotensin-aldosterone system, and increased sympathetic tone. Over time, these responses can lead to ventriculomegaly, cardiomegaly, pulmonary hypertension, ascites, and pulmonary edema (Häggström et al. 2004). As the disease advances, affected dogs may develop clinical signs such as coughing, severe fatigue, exercise intolerance, and, in advanced stages, may experience syncope or even sudden death (Häggström et al. 2004, Harris 2014).

Point-of-care ultrasound (POCUS) is a focused imaging modality characterized by its ease of use, rapid application, and patient safety. It is recommended for addressing specific, clinically urgent questions (Lisciandro 2021). Veterinary practitioners worldwide have adopted the veterinary bedside lung ultrasound exam (VetBLUE) protocol, a POCUS approach designed for rapid, targeted assessment of pulmonary abnormalities, including edema, consolidation, pleural effusion, atelectasis, and pneumothorax. This protocol also facilitates the evaluation of interstitial disease and signs of pulmonary fibrosis, proving particularly valuable in emergency settings. It enables a fast and non-invasive diagnosis that guides immediate therapeutic interventions, especially in dogs with respiratory distress or congestive heart failure (Lisciandro & Lisciandro 2021).

Elastography is an ultrasound-based technique that non-invasively assesses tissue elasticity, emerging as a complementary tool for distinguishing healthy from pathological tissues, thereby aiding early diagnosis and lesion monitoring (Carvalho et al. 2015). Acoustic radiation force impulse (ARFI) elastography is a technology that allows both qualitative and quantitative evaluation of tissue stiffness electronically, without operator dependence (Feliciano et al. 2015, Alves et al. 2024). Elastography has demonstrated diagnostic utility across various clinical applications, particularly in pleural assessment, where its combination with B-mode imaging has aided in differentiating benign from malignant subpleural lesions (Kuo et al. 2021). The technique has also been used in the diagnosis of pulmonary fibrosis and in evaluating pleural stiffness in cases of cardiogenic pulmonary edema (Sperandeo et al. 2009, Wiley et al. 2021). In dogs, ARFI elastography has recently been explored for discriminating between benign and malignant pulmonary lesions (Lima et al. 2025). However, no studies have yet assessed the elasticity of the pneumopleural interface in dogs with heart disease or pulmonary fibrosis.

Based on these principles and considering the challenges in pleuropulmonary assessment of cardiac dogs, this study aimed to evaluate the pneumopleural interface in both healthy and MMVD-affected dogs using B-mode ultrasonography and ARFI elastography. The goal was to identify potential characteristics or predictive values associated with pleuropulmonary alterations and to assess the applicability of ultrasound for the early detection of pleuropulmonary abnormalities in dogs with valvular heart disease.

MATERIALS AND METHODS

Ethical approval. A prospective, observational, case-control study was performed. The study was approved by the Institutional Committee for Animal Care of "Universidade Estadual Paulista 'Júlio de Mesquita Filho'" (Unesp, protocol number 8401/23). The research was conducted using client-owned dogs from the

"Governador Laudo Natel" Veterinary Hospital and dogs from the "Laboratório de Pesquisa em Nutrição e Doenças Nutricionais de Cães e Gatos 'Prof. Dr. Flávio Prada'" ("Professor Doutor Flávio Prada" Canine and Feline Nutrition and Nutritional Diseases Laboratory) at Unesp, Jaboticabal, Brazil.

Dogs were allocated into one of two experimental groups: a sick group (n = 15) and a healthy group (n = 15). The sick group consisted of dogs diagnosed with MMVD by the Cardiology Department of the Veterinary Hospital, based on clinical and echocardiographic examinations. Owners provided voluntary, informed consent for their pets' participation. This group included dogs of various breeds presenting a range of clinical, radiographic, and echocardiographic alterations consistent with an MMVD diagnosis (Keene et al. 2019).

The healthy group consisted of dogs not belonging to high-risk breeds for MMVD (e.g., Cavalier King Charles Spaniels, Dachshunds, Poodles) (Keene et al. 2019). Inclusion criteria were the absence of heart murmurs or abnormal respiratory sounds on auscultation, no evidence of cardiac remodeling, normal pleural and pulmonary surfaces on ultrasound examination, a vertebral heart size (VHS) index below 10.5 (adjusted for breed), and unremarkable lung fields on radiographic examination, in accordance with the American College of Veterinary Internal Medicine consensus guidelines (Keene et al. 2019). Blood examination (hemogram and biochemistry) results were required to be within normal reference ranges. Dogs with any history of respiratory or cardiac disease were excluded.

Radiographic examination. All animals underwent conventional radiographic examination using a Siemens® RG150/100gl X-ray machine. Right and left lateral, ventrodorsal, and dorsoventral projections were obtained to screen for signs of cardiac or pulmonary disease, remodeling, or related sequelae, including tracheal or bronchial abnormalities. The examination also served to exclude primary bronchopulmonary diseases or neoplasms. Cardiac silhouette size was assessed using the VHS index, with values exceeding 10.5 (adjusted for breed) indicating cardiomegaly. The vertebral left atrial size (VLAS) index was also measured, with values greater than three indicating left atrial remodeling (Keene et al. 2019).

Echocardiography. Echocardiographic examination was performed using a Siemens X300 Premium Edition digital ultrasound system equipped with a multi-frequency matrix transducer. Standard right and left parasternal windows were used to evaluate the morphology and function of the left atrium, left ventricle, and mitral valve. All exams were conducted by a board-certified cardiologist to identify the presence or absence of hemodynamic abnormalities, such as pulmonary hypertension or elevated left atrial pressure. B-mode imaging was used to assess wall thickening, echogenicity, and the presence of irregularities or nodules on the valve leaflets, as well as mitral valve prolapse. Color Doppler was applied to visualize mitral regurgitation, identified by a characteristic regurgitant jet into the left atrium.

B-mode pulmonary ultrasonography. Following echocardiographic and radiographic examinations, all dogs underwent pulmonary ultrasonography. An ACUSSON S2000™ (Siemens®, Munich, Germany) ultrasound system with a 9.0–13.0 MHz multi-frequency linear transducer was used. All B-mode images were acquired by a single operator with a minimum of two years of experience, who was blinded to the radiographic, echocardiographic findings and group assignment of each animal. For the transthoracic exam, the transducer was positioned in the intercostal spaces. Shaving was not required; adequate acoustic coupling was achieved using 70% isopropyl alcohol and ultrasound gel. Animals were positioned in sternal, right, or left recumbency, with particular care taken to minimize stress in dogs with respiratory or hemodynamic compromise (Lisciandro 2021). The VetBLUE protocol was followed, systematically examining four thoracic sites on both the right and left hemithorax: the caudodorsal lung lobe (CDLL), perihilar lung lobe (PHLL), medial lung lobe (MDLL), and cranial lung lobe (CRLL) regions. In B-mode, the characteristics of the pleural interface were evaluated, including its thickness, echogenicity, echotexture, and the presence or absence of lung sliding and/or B-lines (Ward et al. 2017). The pneumopleural interface, or "lung line," defined as the hyperechoic, linear interface between the parietal and visceral pleura, was used for thickness measurements. This interface appears as a bright, continuous, and regular line that moves synchronously with respiration (Lisciandro & Lisciandro 2021).

Pulmonary elastography. Following the B-mode examination, ARFI elastography (Virtual Touch™ Tissue Quantification; Siemens®, Germany) was activated for both qualitative and quantitative assessment. Only examinations deemed of high quality by the system's internal quality control, indicated by homogeneous, greenish elastograms, were included. Low-quality, heterogeneous, yellowish images were excluded. Qualitative evaluation was based on the generated elastograms, which provide a color-coded map of tissue stiffness using a fixed SWV scale ranging from 0.5 to 10 m/s. In these maps, blue areas indicate higher elasticity (softer tissue), while red areas indicate lower elasticity (stiffer tissue). The distribution of elasticity was assessed as either homogeneous or heterogeneous. For quantitative analysis, five regions of interest (ROIs), each measuring 1 x 1 mm, were randomly drawn within the pleural tissue at each of the four thoracic sites (CDLL, PHLL, MDLL, CRLL), bilaterally. The software provided an immediate shear wave velocity (SWV) measurement (in m/s) for each ROI. The mean SWV value for each region was calculated for subsequent statistical analysis.

Statistical analysis. Statistical analyses were performed using R software version 3.3.0 (R Foundation for Statistical Computing, Austria). The normality of data distribution was assessed using the Shapiro-Wilk test, and the homogeneity of variances was tested with Bartlett's test to verify assumptions for parametric tests.

Repeated elastography measurements (ROIs) from each pulmonary region were compared using analysis of variance (ANOVA) to determine homogeneity within each region. If no significant differences were found, the median values from each region were used for subsequent analyses. Thickness and elastography measurements from the right and left sides were compared using Student's t-test; if similar, the average of the two sides' values was calculated and used. The mean pleuropulmonary thickness and SWV values for each area were then compared between the sick and healthy groups using Student's t-test. For any variable showing a significant difference, a receiver operating characteristic (ROC) curve analysis was performed using the Wilson/Brown method to estimate its ability to detect pulmonary changes secondary to MMVD. The analysis determined the cutoff value, sensitivity, specificity, and area under the curve (AUC). Data are presented as mean ± standard deviation (SD), with a significance level set at $p < 0.05$.

RESULTS

No complications were observed in any dog during the study, and ultrasonographic examinations yielded images of satisfactory quality for analysis as outlined in the methodology. The study included fifteen healthy Beagle dogs, aged between three and seven years and weighing between 8 and 15 kg, and fifteen dogs in the sick group, aged between eight and 18 years and weighing between 5 and 34 kg (Table 1). The diseased group consisted of mixed-breed dogs (n = 6), Shih Tzu (n = 2), and one dog each of Maltese, American Pitbull Terrier, Dalmatian, Labrador Retriever, Lhasa Apso, Yorkshire Terrier, and Dachshund. Dogs with MMVD were significantly older than healthy dogs ($p < 0.001$), while weight ($p = 0.709$) and gender distribution ($p = 0.275$) were similar between the groups. All animals in the sick group were diagnosed with mitral endocardiosis accompanied by regurgitation. According to the ACVIM consensus guidelines, the classification of MMVD stages was as follows: 7/15 dogs (46.7%) were stage B1, 5/15 (33.3%) were stage B2, and 3/15 (20%) were stage C (Table 1).

On thoracic radiographs of the sick group, cardiomegaly was observed in 3/15 dogs (20%), pulmonary congestion in 3/15 (20%), and bronchopathy in 6/15 (40%), characterized by bronchial wall thickening, hyper- or hypo-inflation of the lungs, increased pulmonary opacity, and associated changes such as atelectasis or bronchiectasis. The remaining 3/15 (20%), classified as stage B1, showed no evident radiographic changes.

On B-mode ultrasonography, B-lines (Fig. 1–4) were identified in 2/15 dogs (13.3%), specifically in the cranial left lung lobe (CRLL) and medial left lung lobe (MDLL). Four B-lines were observed in one dog and three in another, indicating a regional rather than diffuse distribution. Both dogs were classified as stage B2 and had radiographic evidence of bronchial disease, specifically bronchopathy. Their echocardiographic values were as follows: mitral E-wave velocity (0.97 and 1.27 m/s), left atrium-to-aorta ratio (LA/Ao: 1.68 and 2.51), and normalized left ventricular internal diameter in diastole (LVIDDn: 1.77 and 1.91). All animals in the healthy group (Fig. 5) and the remaining dogs in the sick group were negative for the presence of B-lines.

The SWV measurements of the pleuropulmonary interface in the PHLL, MDLL, and CRLL regions were significantly lower ($p < 0.005$) in the sick group than in the control group (Fig. 6-7). The overall mean pleuropulmonary SWV was also significantly lower ($p = 0.009$) in sick animals (3.18 ± 1.09 m/s) than in healthy animals (4.06 ± 0.34 m/s) (Table 2). Pleural thickness was significantly greater ($p = 0.017$) in sick animals (0.91 ± 0.23 cm) than in healthy animals (0.74 ± 0.11 cm), specifically in the MDLL region (Fig. 8–11). The overall mean pleural thickness was also significantly greater ($p = 0.022$) in sick animals (0.88 ± 0.21 cm) compared to healthy animals (0.73 ± 0.04 cm) (Table 2). SWV and thickness measurements in other evaluated regions (CDLL SWV and thickness, PHLL thickness, and CRLL thickness) showed no significant differences ($p > 0.050$) between the groups.

While pleural thickness measurements alone did not allow for a significant ($p = 0.071$) identification of alterations in the sick group, the overall mean pleuropulmonary SWV proved to be an effective indicator (Fig. 12). A cutoff value of SWV < 3.71 m/s ($p = 0.004$) identified these alterations with a sensitivity of 80% and a specificity of 86.67%. The diagnostic performance characteristics (p-value, cutoff value, sensitivity, specificity, likelihood ratio, and AUC) for each studied area and variable are detailed in Table 3.

DISCUSSION

The results of this study partially supported our initial hypotheses. While significant differences were identified in both B-mode and elastography evaluations between healthy dogs and those with MMVD, only elastography demonstrated a reliable capacity to detect pleuropulmonary alterations associated with the disease.

B-lines were observed in only two dogs, both classified with stage B2 MMVD. These animals also exhibited a bronchointerstitial pattern on thoracic radiography, a finding often associated with airway inflammation from allergic or infectious diseases, but which can also be a consequence of peribronchial edema secondary to cardiac dysfunction (Thrall 2018). In ultrasonography, B-lines are a nonspecific sign of alveolar-interstitial syndrome, commonly linked to edema, and are typically assessed based on their regional distribution (Lisciandro 2021). Previous studies have documented B-lines in mid-thoracic and cranial windows of dogs with left heart failure (Lisciandro et al. 2014). In the present cases, their presence suggests a possible inflammatory condition or early cardiogenic pulmonary edema. According to established criteria, a hemithorax site is

considered positive when more than three B-lines are present, and animals with two or more positive sites are indicative of acute cardiogenic edema (Ward et al. 2017). Although the dogs in this study had three and four B-lines, respectively, they were restricted to a single hemithorax, potentially representing a very early stage of disease. The absence of B-lines in stage C dogs was unexpected but may be attributed to the fact that all were receiving pharmacological treatment, which could have mitigated overt edema.

This study also identified increased pleural thickness in the medial lung lobe (MDLL) region of dogs with MMVD. To our knowledge, this finding has not been previously described in dogs with cardiac disease. We propose that this thickening may be related to underlying inflammatory processes. Analogous findings in human medicine occur in conditions such as pleuritis (Larson 2009), where pleural irritation triggers a response involving thickening, hypervascularization, and inflammation, including dilation of lymphatic channels and proliferation of elastic tissues (Rodriguez-Panadero & Antony 1997, Marsico et al. 2001). Furthermore, pleural thickening observed on computerized tomography (CT) scans in human patients with hydrostatic pulmonary edema is a recognized feature of early pulmonary congestion (Lee et al. 2021) and can indicate a diffuse inflammatory state in patients with heart failure (Evison & Barber 2015). Consequently, the increased pleural thickness found in our study may represent early inflammation at the pleuropulmonary interface in dogs with MMVD.

A key finding was a significant reduction in pleural stiffness, quantified by lower SWV, in the medial and cranial lung lobe regions of sick dogs. In human medicine, elastography is used to differentiate malignant pleural effusions from benign conditions (Hassan et al. 2020, Taymour et al. 2024) and to detect increased stiffness in fibrotic lung diseases (Nouvenne et al. 2022, Vargas-Ursúa et al. 2024). However, inflammatory processes may reduce tissue elasticity before fibrosis develops, particularly due to increased tissue water content (Chen et al. 2024). This mechanism may explain the reduced SWV observed in dogs with MMVD. Although age differences between groups should be considered a potential confounding factor, aging and fibrotic pulmonary diseases are generally associated with increased, rather than reduced, tissue stiffness (Reinero 2019a, 2019b). In addition, qualitative elastographic evaluation did not reveal consistent color patterns associated with pleural thickening on B-mode ultrasonography; therefore, interpretation was based primarily on quantitative SWV measurements.

Our findings are consistent with a recent veterinary study (Lima et al. 2025), which reported lower elastography values in atelectatic lung lesions compared to solid masses or consolidations. While that study focused on pulmonary lesions and ours on the pleuropulmonary interface in cardiac patients, both conclude that a reduction in tissue stiffness can be a marker of pathology. This reinforces the value of elastography as a sensitive tool for detecting structural changes, although the specific pathophysiological meaning of a decreased SWV requires further investigation. Previous studies (Lima et al. 2025) emphasized the utility of elastography for characterizing lesions, especially with effusion, and our work extends its potential application to the evaluation of pleural abnormalities in a common cardiac disease.

This study has several limitations. The sample size was small, and the groups were not age-matched, with dogs in the sick group being significantly older. While this age distribution is consistent with the known epidemiology of MMVD (Keene et al. 2019), future studies with larger, age-controlled cohorts are encouraged. The cross-sectional design also prevented longitudinal monitoring to observe the progression of bronchopathies or edema and to assess the impact of ongoing medical therapy. In addition, body weight may have influenced elastographic acquisition in some animals, particularly in larger dogs with thicker muscular and adipose layers, potentially affecting acoustic penetration and color-mapping quality. Respiratory motion, especially in panting dogs, may also have interfered with measurement stability.

CONCLUSION

This study reveals the promising applicability of acoustic radiation force impulse (ARFI) elastography for evaluating pleuropulmonary interface elasticity in dogs with myxomatous mitral valve disease (MMVD). The technique emerged as a highly sensitive and specific diagnostic tool for identifying pleural abnormalities, particularly in the medial lung lobe (MDLL) and cranial lung lobe (CRLL) regions, showing great promise for the early detection of pathological changes in this dog population.

Acknowledgments.- The authors would like to thank “Fundação de Amparo à Pesquisa do Estado de São Paulo” (FAPESP) (grant process numbers: 2022/07366-0) and “Conselho Nacional de Desenvolvimento Científico e Tecnológico” (CNPq) for funding the research (productivity scholarship: 305182/2020-0), and owners and breeders of the dogs participating in this study.

Conflict of interest statement.- The authors declare that they have no conflicts of interest.

Credit author statement.- Brenda S.P. Miranda: Conceptualization, Data curation, Formal analysis, Funding acquisition, Investigation, Methodology, Validation, Visualization, Writing – original draft. Bruna B. Lima, Rafael K. Carneiro, Danuta P. Doiche, Giovanna S.M. Feliciano: Investigation, Methodology, Validation. Gabriela C.L.

Evangelista and Ricardo A.R. Uscategui: Formal analysis, Supervision, Validation, Visualization, Writing – original draft, Writing – review & editing. Marcus A.R. Feliciano: Conceptualization, Funding acquisition, Methodology, Project administration, Resources, Supervision, Visualization, Writing – original draft, Writing – review & editing. All authors have read and approved the manuscript.

Data availability statement.- Data supporting the results are available from the corresponding author upon reasonable request.

Editor-in-Chief.- Fabiano José Ferreira de Sant'Ana.

REFERENCES

Alves ACA, Maronezi MC, Pazzini JM, Cruz ICK, Gomes DR, Uchoa AS, Ramos DJ, Nardi AB, Salazar DVV, Feliciano MAR. ARFI (Acoustic Radiation Force Impulse) elastography and B-mode ultrasonography of the adrenal glands in healthy dogs of different ages. Arq Bras Med Vet Zootec 2024; https://doi.org/10.1590/1678-4162-13082

Carvalho F, Cintra TCF, Chammas MC. Elastography: principles and considerations for clinical research in veterinary medicine cibele. J Vet Med Anim Health 2015; https://academicjournals.org/journal/JVMAH/article-full-text-pdf/BDEC2E750556.pdf

Chen Z, Wang Y, Ying MTC, Su Z, Han X, Gunda ST. Association of renal elasticity evaluated by real-time shear wave elastography with renal fibrosis in patients with chronic kidney disease. Br J Radiol 2024; https://doi.org/10.1093/bjr/tqad030

Evison M, Barber P. Diffuse pleural thickening following heart failure-related pleural effusions in an asbestos exposed patient. Int J Occup Environ Health 2015; https://doi.org/10.1179/2049396714Y.0000000104

Feliciano MAR, Maronezi MC, Simões APR, Uscategui RR, Maciel GS, Carvalho CF, Canola JC, Vicente WRR. Acoustic radiation force impulse elastography of prostate and testes of healthy dogs: preliminary results. J Small Anim Pract 2015; https://doi.org/10.1111/jsap.12323

Häggström J, Pedersen HD, Kvart C. New insights into degenerative mitral valve disease in dogs. Vet Clin North Am Small Anim Pract 2004; https://doi.org/10.1016/j.cvsm.2004.05.002

Harris J. Advanced degenerative mitral valve disease and congestive heart failure in dogs. Companion Anim 2014; https://doi.org/10.12968/coan.2014.19.4.196

Hassan M, Mercer RM, Rahman NM. Thoracic ultrasound in the modern management of pleural disease. Eur Respir Rev 2020; https://doi.org/10.1183/16000617.0136-2019

Keene BW, Atkins CE, Bonagura JD, Fox PR, Häggström J, Fuentes VL, Oyama MA, Rush JE, Stepien R, Uechi M. ACVIM consensus guidelines for the diagnosis and treatment of myxomatous mitral valve disease in dogs. J Vet Intern Med 2019; https://doi.org/10.1111/jvim.15488

Kuo Y-W, Chen Y-L, Wu H-D, Chien Y-C, Huang C-K, Wang H-C. Application of transthoracic shear-wave ultrasound elastography in lung lesions. Eur Respir J 2021; https://doi.org/10.1183/13993003.02347-2020

Larson MM. Ultrasound of the thorax (noncardiac). Vet Clin North Am Small Anim Pract 2009; https://doi.org/10.1016/j.cvsm.2009.04.006

Lee EY, Jenkins KJ, Vargas SO, Callahan R, Park HJ, Gauthier Z, Winant AJ. Thoracic multidetector computed tomography angiography of primary pulmonary vein stenosis in children: evaluation of characteristic extravascular findings. J Thorac Imaging 2021; https://doi.org/10.1097/RTI.0000000000000590

Lima BB, Carneiro RK, Miranda BSP, Gasser B, Aires LPN, Terrabuio VMTC, Uscategui RAR, Lacreta Junior ACC, Doiche DP, Evangelista GCL, Feliciano MAR. Acoustic radiation force impulse elastographic study of lung lesions in dogs. Vet Radiol Ultrasound 2025; https://doi.org/10.1111/vru.70031

Lisciandro GR, Fosgate GT, Fulton RM. Frequency and number of ultrasound lung rockets (B-lines) using a regionally-based lung ultrasound examination named Vet BLUE (veterinary bedside lung ultrasound exam) in dogs with radiographically normal lung findings. Vet Radiol Ultrasound 2014; https://doi.org/10.1111/vru.12122

Lisciandro GR, Lisciandro SC. POCUS: Vet BLUE – Clinical Integration, p.459-507. In: Lisciandro GR. Point-of-care Ultrasound Techniques for the Small Animal Practitioner. 2021; https://doi.org/10.1002/9781119461005.ch23

Lisciandro GR. Point-of-care Ultrasound Techniques for the Small Animal Practitioner. 2021; https://doi.org/10.1002/9781119461005

Marsico GA, Haddad R, Carvalho CES, Assis PG, Martinelli Júnior I, Martins MG. Efeitos do sulfato de bário na cavidade pleural de ratos. Rev Col Bras Cir 2001; https://doi.org/10.1590/S0100-69912001000500009

Nouvenne A, Zanichelli I, Cerundolo N, Milanese G, Sverzellati N, Rendo M, Ridolo E, Scarlata S, Meschi T, Ticinesi A. Thoracic ultrasound strain elastosonography as a noninvasive biomarker of Chronic Obstructive Pulmonary Disease-Associated lung injury: a feasibility study. Respiration 2022; https://doi.org/10.1159/000525864

Reinero C. Interstitial lung diseases in dogs and cats part I: the idiopathic interstitial pneumonias. Vet J 2019a; https://doi.org/10.1016/j.tvjl.2018.11.010

Reinero C. Interstitial lung diseases in dogs and cats part II: known cause and other discrete forms. Vet J 2019b; https://doi.org/10.1016/j.tvjl.2018.11.011

Rodriguez-Panadero F, Antony VB. Pleurodesis: state of the art. Eur Respir J 1997; https://doi.org/10.1183/09031936.97.10071648

Sperandeo M, Varriale A, Sperandeo G, Filabozzi P, Piattelli ML, Carnevale V, Decuzzi M, Vendemiale G. Transthoracic ultrasound in the evaluation of pulmonary fibrosis: our experience. Ultrasound Med Biol 2009; https://doi.org/10.1016/j.ultrasmedbio.2008.10.009

Taymour TA, Mohamed LSW, El Hinnawy YH, El-Mageed MRA. Can ultrasound shear wave elastography differentiate between malignant and benign pleural effusions? Egypt J Radiol Nucl Med 2024; https://doi.org/10.1186/s43055-024-01209-y

Thrall DE. Textbook of Veterinary Diagnostic Radiology. 7th ed. St Louis: Elsevier; 2018.

Vargas-Ursúa F, Ramos-Hernández C, Pazos-Area LA, Fernández-Granda I, Rodríguez-Otero I, Gómez-Corredoira E, Pintos-Louro M, Fernández-Villar A. Current evidence for lung ultrasound elastography in the field of pneumology: a systematic review. ERJ Open Res 2024; https://doi.org/10.1183/23120541.00081-2024

Ward JL, Lisciandro GR, Keene BW, Tou SP, DeFrancesco TC. Accuracy of point-of-care lung ultrasonography for the diagnosis of cardiogenic pulmonary edema in dogs and cats with acute dyspnea. J Am Vet Med Assoc 2017; https://doi.org/10.2460/javma.250.6.666

Wiley BM, Zhou B, Pandompatam G, Zhou J, Kucuk HO, Zhang X. Lung ultrasound surface wave elastography for assessing patients with pulmonary edema. IEEE Trans Biomed Eng 2021; https://doi.org/10.1109/TBME.2021.3072891

Figures

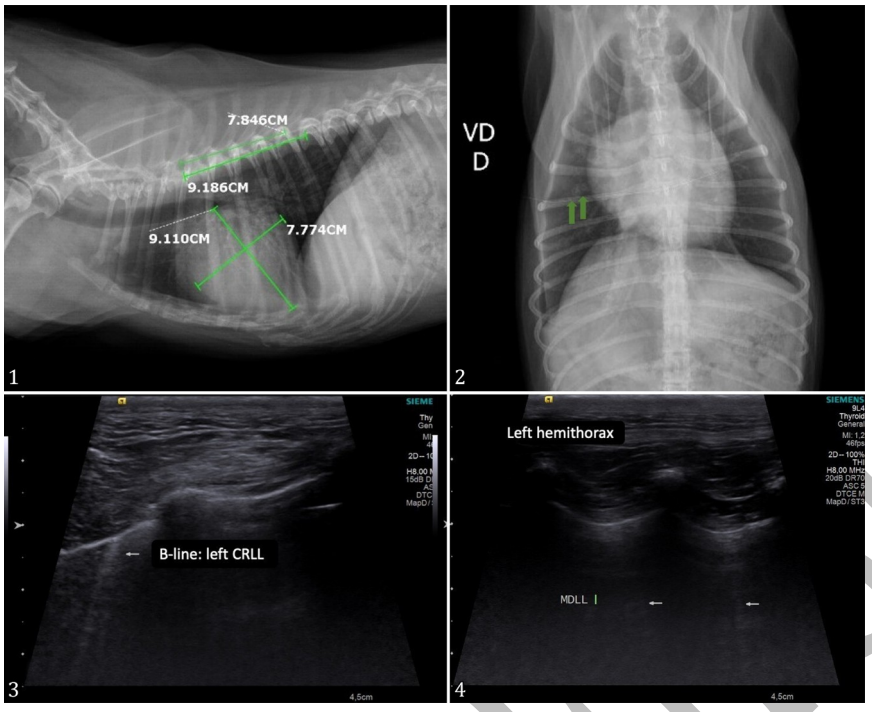

Fig. 1–4. (**1**-**2**) Radiographic and (**3**-**4**) ultrasonographic thoracic images of a dog with myxomatous mitral valve disease (MMVD) sick group. (**1**) Right lateral projection showing the cardiac silhouette occupying 3.3 intercostal spaces, with a vertebral heart size (VHS) of 9.7 measured by green tracings. (**2**) Ventrodorsal projection with the bronchointerstitial pattern (green block arrows). B-mode ultrasonographic evaluation of the (**3**) cranial lung lobe (CRLL) and (**4**) medial lung lobe (MDLL) thoracic site of the same patient showing the presence of B-lines (white arrow in Fig. 3 and 4) originating from the pleural interface.

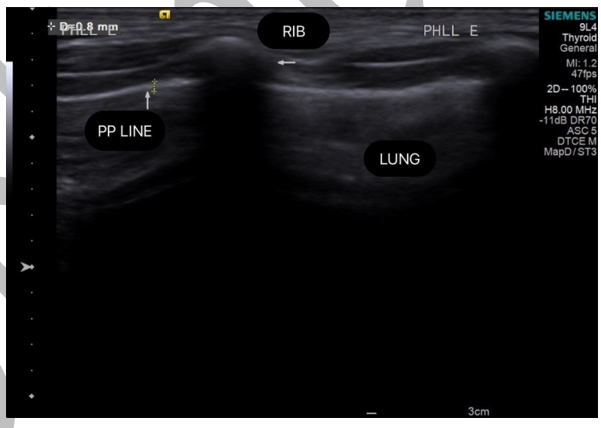

Fig. 5. B-mode ultrasonographic image of the left perihilar lung lobe (PHLL) thoracic site of a dog from the healthy group. The pleuropulmonary line (PP) is visible as a hyperechoic interface (measured between yellow calipers), the rib appears as a curved structure producing acoustic shadowing (white arrow labeled as rib), and the normal lung is visualized by the presence of A-lines (labeled as lung), with reverberation artifacts seen as parallel echogenic lines in the horizontal direction.

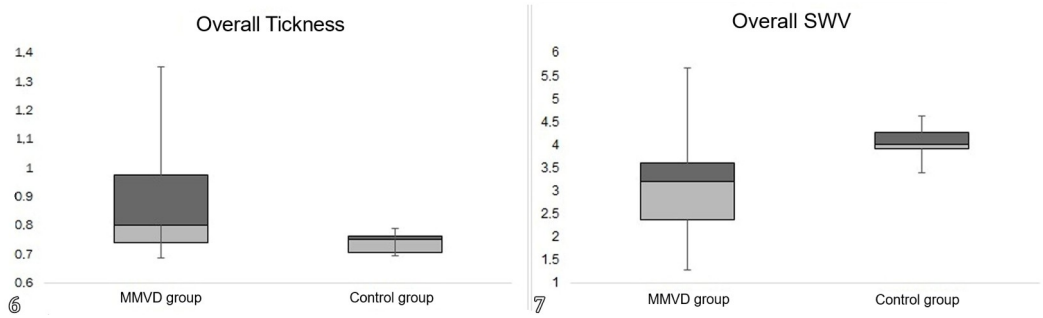

Fig. 6–7. Graphic representation boxplot of (**6**) overall pleural thickness evaluated by B-mode ultrasound and (**7**) overall pleuropulmonary shear wave velocity (SWV) evaluated by elastography, in dogs with myxomatous mitral valve disease (MMVD) group compared with the healthy dogs control group.

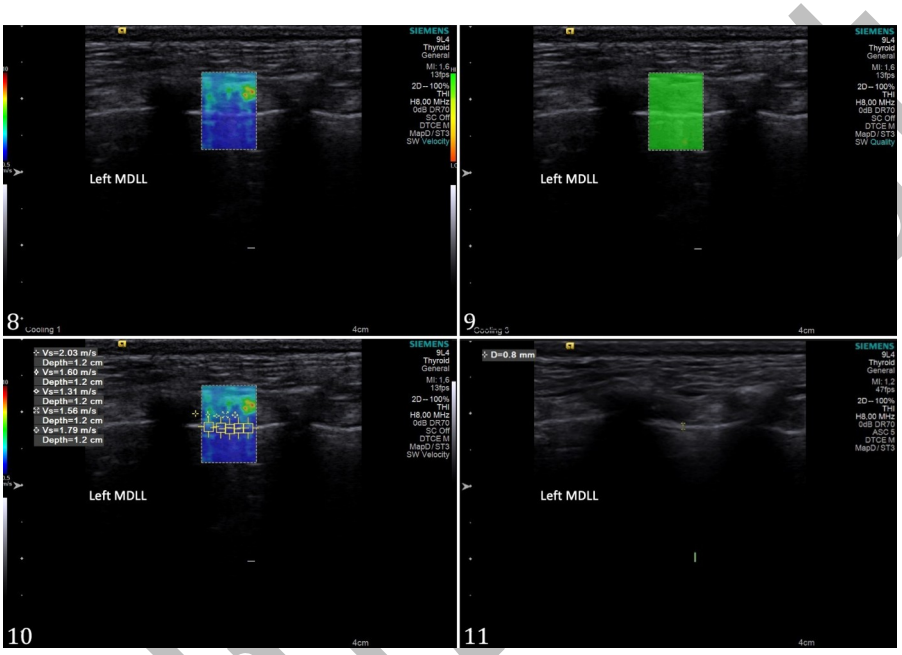

Fig. 8–11. (**8**-**10**) Acoustic radiation force impulse (ARFI) elastography and (**11**) B-mode ultrasound images at the left medial lung lobe (MDLL) thoracic site of a dog with stage C of myxomatous mitral valve disease (MMVD). (**8**) Qualitative study showing the color elastogram, cold colors represent more elastic areas, and warm colors represent stiffer areas. (**9**) Elastogram quality assessment indicating high quality due to the homogeneity of the greenish color. (**10**) quantitative assessment of the pleuropulmonary interface with a shear wave velocity (SWV) of 1.54 m/s. (**11**) B-mode ultrasound demonstrating pleural thickness of 0.8 mm (measured between yellow calipers).

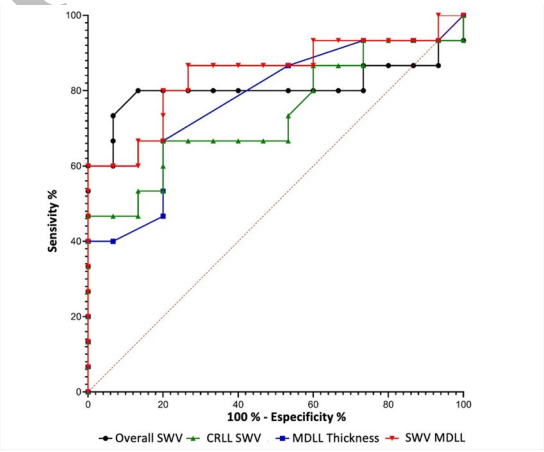

Fig. 12. Receiver operating characteristic (ROC) curves comparing the diagnostic sensitivity and specificity of the different ultrasound and elastography parameters studied in the prediction of pleural abnormalities in dogs with myxomatous mitral valve disease (MMVD).

Table 1. Demographic data (range) for healthy dogs and dogs with the myxomatous mitral valve disease (MMVD) grouped according to the ACVIM stage

Variable	Healthy	Stage B1	Stage B2	Stage C
Number	15	7	5	3
Female/male	11/4	4/3	3/2	1/2
Age (years)	(3 – 7)	(8 – 12)*	(12 – 16)*	(11 – 14)*
Body weight (kg)	(5.1 – 14.9)	(6.4 – 22)	(5.5 – 28.5)	(8.0 – 14.0)

* $p < 0.001$ compared with healthy dogs.

Table 2. Mean ± standard deviation (SD) and comparative (t-Student) *p*-value of B-mode (pleural thickness cm) and elastography (pleuropulmonary shear wave velocity (SWV) m/s) examination in healthy dogs (n = 15) and sick dogs (n = 15) with myxomatous mitral valve disease (MMVD)

Parameter	Mean	*p*-value
Overall SWV (m/s)		
Healthy group	4.62 ± 0.34	0.009*
Sick group	3.18 ± 1.09	
PHLL SWV (m/s)		
Healthy group	4.14 ± 0.68	0.017*
Sick group	3.17 ± 1.27	
CDLL SWV (m/s)		
Healthy group	4.05 ± 0.72	0.128
Sick group	3.37 ± 1.51	
MDLL SWV (m/s)		
Healthy group	4.09 ± 0.59	0.001*
Sick group	2.93 ± 0.99	
CRLL SWV (m/s)		
Healthy group	3.96 ± 0.48	0.038*
Sick group	3.27 ± 1.11	
Overall thickness (cm)		
Healthy group	0.73 ± 0.42	0.022*
Sick group	0.88 ± 0.21	
PHLL Thickness (cm)		
Healthy group	0.74 ± 0.09	0.08
Sick group	0.86 ± 0.25	
CDLL Thickness (cm)		
Healthy group	0.74 ± 0.09	0.057
Sick group	0.89 ± 0.28	
MDLL Thickness (cm)		
Healthy group	0.74 ± 0.11	0.017*
Sick group	0.91 ± 0.23	
CRLL Thickness (cm)		
Healthy group	0.73 ± 0.08	0.054
Sick group	0.83 ± 0.18	

PHLL = Perihilar pulmonary lobe region, CDLL = caudodorsal pulmonary lobe region, MDLL = medial pulmonary lobe region, CRLL = cranial pulmonary lobe region, n = number of animals evaluated; *Significant by t-Student ($p < 0.05$).

Table 3. Diagnostic performance variables of pleuropulmonary shear wave velocity (SWV m/s) evaluated by elastography and pleural thickness (cm) evaluated by B-mode ultrasound, of different areas of pleuropulmonary surface evaluated in dogs with myxomatous mitral valve disease, compared with healthy dogs

Parameter	*p*-value	Cutoff	Sensibility (%)	Specificity (%)	Likelihood ratio	AUC (%)
Overall SWV	0.0042	< 3.715	80.0	86.7	6.00	0.807
PHLL SWV	0.2902	N/A	N/A	N/A	N/A	N/A
MDLL SWV	0.0013	< 3.540	80.0	80.0	4.00	0.844
CRLL SWV	0.0279	< 3.660	66.6	80.0	3.33	0.736
Overall thickness	0.0712	N/A	N/A	N/A	N/A	N/A
MDLL thickness	0.0014	> 0.775	66.6	80.0	3.33	0.771

AUC = Area under the curve, PHLL = perihilar pulmonary lobe region, MDLL = medial pulmonary lobe region, CRLL = cranial pulmonary lobe region, N/A = not applicable.